

Neuroprotective Effect of *N*-Cyclohexylethyl-[A/G]-[D/E]-X-V Peptides on Ischemic Stroke by Blocking nNOS–CAPON InteractionYajuan Qin,^{*,†} Lingling Feng,[†] Xin Fan, Liping Zheng, Yu Zhang, Lei Chang, and Tingyou Li^{*}Cite This: *ACS Chem. Neurosci.* 2021, 12, 244–255

Read Online

ACCESS |

Metrics & More

Article Recommendations

Supporting Information

ABSTRACT: The protein–protein interaction between neuronal nitric oxide synthases (nNOS) and the carboxy-terminal PDZ ligand of nNOS (CAPON) is a potential target for the treatment of ischemic stroke. Our previous study had identified ZLc-002 as a promising lead compound for inhibiting nNOS–CAPON coupling. To find better neuroprotective agents disrupting the ischemia-induced nNOS–CAPON interaction, a series of *N*-cyclohexylethyl-[A/G]-[D/E]-X-V peptides based on the carboxy-terminal tetrapeptide of CAPON was designed, synthesized, and evaluated in this study. Herein, we reported an affinity-based fluorescence polarization (FP) method using 5-carboxyfluorescein (5-FAM) labeled CAPON (496–506) peptide as the probe for high-throughput screening of the small-molecule inhibitors of the PDZ domain of nNOS. *N*-Cyclohexylethyl-ADAV displayed the most potent affinity for the nNOS PDZ domain in the FP and isothermal titration calorimetry (ITC) ($\Delta H = -1670 \pm 151.0$ cal/mol) assays. To improve bioavailability, lipophilicity, and membrane permeability, the Asp methylation was employed to get *N*-cyclohexylethyl-AD(OMe)AV, which possesses good blood–brain barrier (BBB) permeability *in vitro* parallel artificial membrane permeability assay (PAMPA)–BBB ($P_e = 6.07$ cm/s) and *in vivo* assays. In addition, *N*-cyclohexylethyl-AD(OMe)AV (10 mg/kg body weight, i.v., immediately after reperfusion) substantially reduced infarct size in rats, which was measured 24 h after reperfusion and subjected to 120 min of middle cerebral artery occlusion (MCAO).

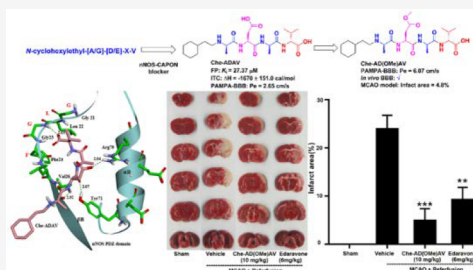
KEYWORDS: nNOS–CAPON interaction blockers, anti-ischemic stroke, FP, ITC, MCAO

1. INTRODUCTION

Ischemic stroke is a major public health problem that leads to high rates of death and long-term disability in adults.¹ At the present, research on stroke targets mainly includes calcium antagonists,² glutamate release inhibitors, γ -amino butyric acid (GABA) receptor agonists,³ free radical scavengers,⁴ MMP-9 inhibitors,⁵ *N*-methyl-D-aspartate receptor (NMDAR) antagonists,⁶ NOS inhibitors,^{7,8} nNOS-PSD95 PPI,⁹ neuronal nitric oxide synthases (nNOS)–carboxy-terminal PDZ ligand of nNOS (CAPON) interaction blockers,¹⁰ etc. But unfortunately, no other new effective drug for ischemic stroke has been approved by the Food and Drug Administration (FDA), currently, since the recombinant tissue plasminogen activator (tPA) was licensed in 1996.¹¹ However, only 2–5% stroke patients received rtPAs treatment due to its short therapeutic time window.¹² Ederavone, a free radical scavenger, was approved by the Japanese Ministry of Health in 2001 for the treatment of acute ischemic stroke (AIS). It was reported that combination therapy with edaravone and endovascular reperfusion therapy was significantly associated with greater functional independence at hospital discharge, lower in-hospital mortality, and reduced intracranial hemorrhage in AIS patients.¹³ However, the potential adverse effects of edaravone were reported in some cases, such as acute renal failure (ARF), fulminant hepatitis, and disseminated intra-

vascular coagulation (DIC).¹⁴ Therefore, it is critical to explore a new, effective, safe, and extended therapeutic time window drug to treat the ischemic stroke.

Reportedly, a stroke enhances the nNOS–CAPON interaction in the acute phase.¹⁰ Studies have shown that inhibiting the coupling of nNOS–CAPON has a neuroprotective effect. In 2013, Courtney et al. reported that a cell-permeable peptide TAT-GESV, which competes for nNOS PDZ domain interacting with CAPON, can inhibit excitatory toxicity signals and damage in cultured neurons and animal models of cerebral ischemia.¹⁰ The interaction between the nNOS-PDZ domain and CAPON mediates the recruitment of and requirement for CAPON in p38MAPK-dependent excitotoxic neuronal death. In 2019, we published that a stroke increased nNOS–CAPON association in the peri-infarct cortex in the delayed period.¹⁵ In our previous work, we reported a potent blocker ZLc-002(*N*-(2-carbomethoxyacetyl)-D-valine methyl ester) of nNOS–CAPON binding in



Received: November 18, 2020

Accepted: December 10, 2020

Published: December 23, 2020

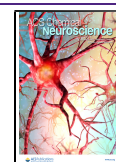
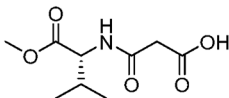


Table 1. List of Designed and Synthesized Compounds

Compounds	Structure	Inhibition ratio (%)
ZLc-002-1		34.00
Che-AEAV	<i>N</i> -Cyclohexylethyl-NH-Ala-Glu-Ala-Val-COOH	65.87
Che-AEWV	<i>N</i> -Cyclohexylethyl-NH-Ala-Glu-Trp-Val-COOH	78.45
Che-ADWV	<i>N</i> -Cyclohexylethyl-NH-Ala-Asp-Trp-Val-COOH	86.61
Che-AEFV	<i>N</i> -Cyclohexylethyl-NH-Ala-Glu-Phe-Val-COOH	0.77
Che-ADAV	<i>N</i> -Cyclohexylethyl-NH-Ala-Asp-Ala-Val-COOH	96.38
Che-AEIV	<i>N</i> -Cyclohexylethyl-NH-Ala-Glu-Ile-Val-COOH	12.79
Che-ADIV	<i>N</i> -Cyclohexylethyl-NH-Ala-Asp-Ile-Val-COOH	87.44
Che-GDAV	<i>N</i> -Cyclohexylethyl-NH-Gly-Asp-Ala-Val-COOH	82.99
Che-GDPV	<i>N</i> -Cyclohexylethyl-NH-Gly-Asp-Pro-Val-COOH	85.04
Che-GDLV	<i>N</i> -Cyclohexylethyl-NH-Gly-Asp-Leu-Val-COOH	97.24
Che-GDFV	<i>N</i> -Cyclohexylethyl-NH-Gly-Asp-Phe-Val-COOH	67.83
Che-GDWV	<i>N</i> -Cyclohexylethyl-NH-Gly-Asp-Trp-Val-COOH	94.84

cultured hippocampal neurons from ICR mice in *Nature Medicine*.¹⁶ ZLc-002 improved motor function in transient middle cerebral artery occlusion (tMCAO) mice.¹⁵ nNOS–CAPON interaction could serve as a novel pharmacological target for functional restoration after a stroke, and it could serve as a new therapeutic target in the delayed phase for stroke recovery.¹⁵

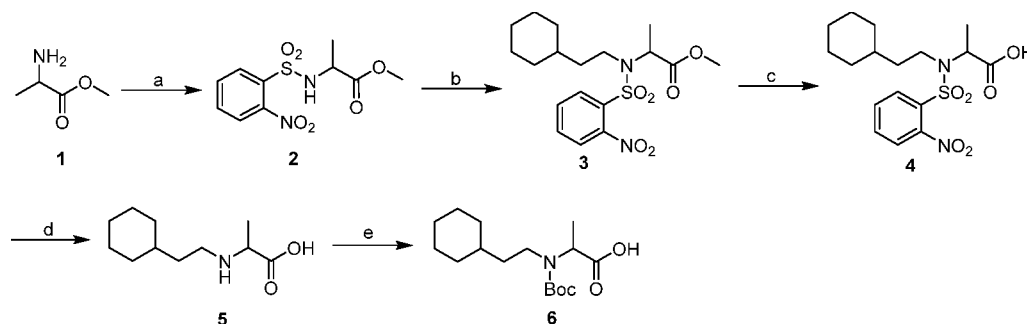
CAPON is a natural ligand of nNOS and is able to bind to the pocket constituted by the α B helix and β B fold of the nNOS PDZ domain through its carboxy-terminal tetrapeptide EIIV.¹⁷ The binding site is a shallow and long groove containing the binding pocket of the conserved sequence GLGF (Gly21, Leu 22, Gly23, Phe24).¹⁸ The *N*-cyclohexylethyl group (-Che) could increase the binding potency with PDZ domains, plasma stability, and cell permeation.^{19,20} On the basis of the carboxy-terminal tetrapeptide of CAPON and our previous research, we designed a series of *N*-cyclohexylethyl-tetrapeptides (Che-tetrapeptide) to uncouple nNOS and CAPON by competitively binding to the GLGF regional pocket of nNOS PDZ domain.

Here, we have established a method for the high-throughput screening assay based on fluorescence polarization (FP) for testing the binding affinities of compounds to nNOS PDZ domain. 5-Carboxyfluorescein (5-FAM) labeled CAPON (496–506) terminalpeptide was synthesized and employed as the probe (5-FAM-KV-14). GST-nNOS PDZ was expressed, purified, and identified as the protein. Isothermal titration calorimetry (ITC) was used to fit the binding process of 5-FAM-KV-14 and GST-nNOS_{1–133} protein to verify that the binding was a typical single-point binding. In addition, we optimized the experimental conditions, such as the optimal

concentration of the protein and probe, incubation time, dimethyl sulfoxide (DMSO) tolerance and stability, and so on, and demonstrated the feasibility of applying this method for the high-throughput screening of inhibitors binding to the nNOS PDZ domain. The affinities of compounds for nNOS PDZ domain were preliminary and secondary screened by FP assay. Subsequently, ITC was employed to analyze the binding activities of nNOS PDZ and two compounds. The results of ITC correlated well with the data of FP experiment. To improve the bioavailability, lipophilicity, and membrane permeability, the Asp methylation was employed to get Che-AD(OMe)AV, which possesses good blood–brain barrier (BBB) permeability *in vitro* parallel artificial membrane permeability assay (PAMPA)-BBB and *in vivo* assays. In addition, Che-AD(OMe)AV (10 mg/kg body weight, i.v., immediately after reperfusion) substantially reduced the infarct size in rats, which was measured 24 h after reperfusion subjected to 120 min of MCAO.

2. RESULTS AND DISCUSSION

2.1. Design and Synthesis. PDZ domains typically interacted with the carboxyl terminus of their binding protein.²¹ It was generally acknowledged that the first (P^0) and the third (P^{2-}) amino acids of the binding ligand (counting from the C-terminal amino acid) were considered quite important for affinity with the PDZ domain.^{22,23} Val in the first position (P^0) was critical for affinity for nNOS PDZ and CAPON. Because if the Val (P^0) on the carboxyl terminal of CAPON was substituted to other amino acids, even a close relative Ala, the binding activities with nNOS were almost completely disappeared. The carboxyl at the side chain of the

Scheme 1. Synthesis of Compound 6^a

^aReagents and conditions: (a) 2-nitrobenzenesulfonyl (Nos) chloride, Et₃N, THF/H₂O, 0 °C–rt, 2 h; (b) 2-cyclohexylethan-1-ol, DIAD, Ph₃P; DMF, 0 °C–rt, overnight; (c) NaOH, MeOH, rt, overnight; (d) sodium thiophenolate, DMF, rt, overnight; (e) Et₃N, (Boc)₂O, 1,4-dioxane, rt.

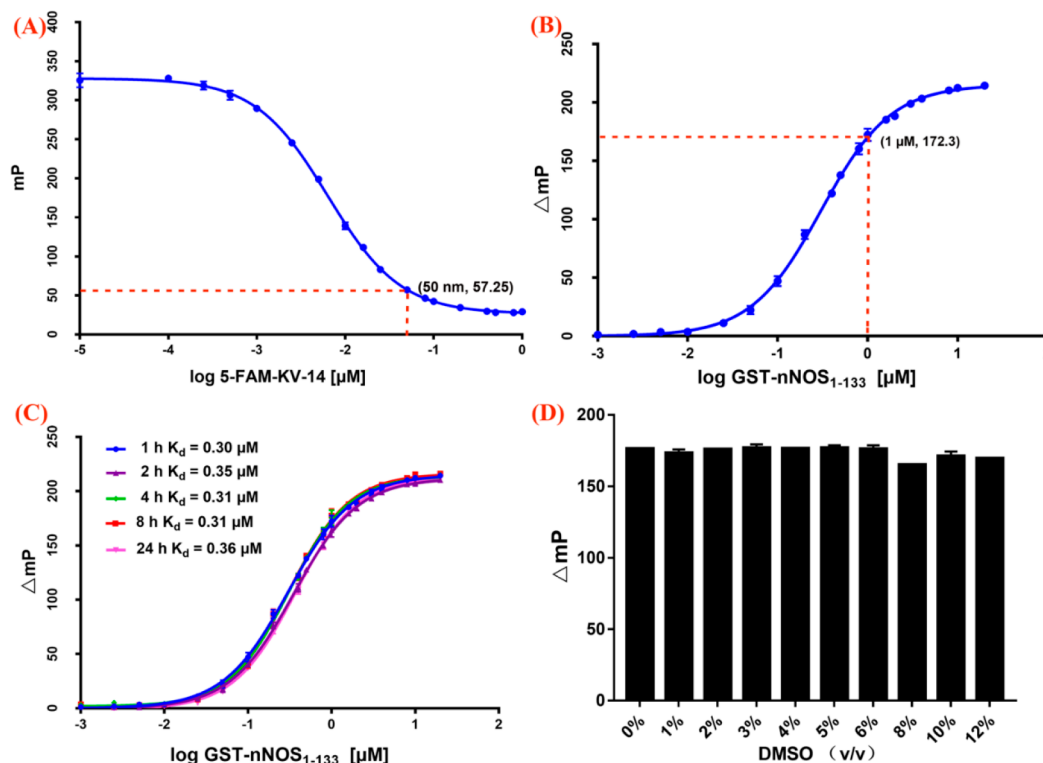


Figure 1. (A) Determination of the optimal concentration of the free probe for fluorescence polarization assay by varying the concentration of 5-FAM-KV-14 (0.01 nM–5 μM). (B) Optimization of the binding concentration for GST-nNOS₁₋₁₃₃ using a 50 nM probe and increasing the concentrations of GST-nNOS₁₋₁₃₃ protein (from 1 nM to 20 μM). At the concentration of 1 μM, the binding of 5-FAM-KV-14 and GST-nNOS₁₋₁₃₃ was saturated. (C) Stability of binding experiments over a 24 h period. Binding experiments were performed using a 50 nM probe and increasing the concentrations of GST-nNOS₁₋₁₃₃ protein (from 1 nM to 20 μM). (D) Effect of DMSO on the binding experiments (0–12%).

P²⁻ amino acid could form a hydrogen-bond interaction with the phenolic hydroxyl of Tyr-71 on the nNOS PDZ domain.²⁴ So Asp and Glu, with carboxyl side chains, were selected in the P²⁻ position in this study. The results of peptides library screening for the nNOS PDZ domain showed that the occurrence rate of acidic and basic amino acids in the P¹⁻ site was extremely low. However, the total occurrence rate of lipophilic amino acids, such as Ala, Leu, Ile, Phe, Pro, and Trp, was 76%, indicating that a lipophilic amino acid is favorable at this position.²⁵ Considering the optimal sequence “-G-[D/E]-x-v” screened by a peptide library, steric hindrance, and polarity of the tetrapeptide, Gly and Ala with small side chains were selected at the P³⁻ location. The *N*-cyclohexylethyl group could increase the binding potency with PDZ domains, plasma stability, and cell permeation. Therefore, on the basis of the

carboxy-terminal tetrapeptide of the CAPON and our previous research, we designed and synthesized a series of *N*-cyclohexylethyl-[G/A]-[D/E]-X-V peptides (Table 1) to uncouple nNOS and CAPON by competitively binding to the GLGF regional pocket of the nNOS PDZ domain.

The synthetic route for the preparation of compounds *N*-Boc-*N*-Che-Val-OH (6) is shown in Scheme 1. Compound 2 was synthesized by the treatment of H-Ala-OMe with 2-nitrobenzenesulfonyl chloride in the presence of triethylamine in dry DCM. Then, intermediate 2 was used in the subsequent Mitsunobu reaction with 2-cyclohexylethan-1-ol mediated by diisopropyl azodicarboxylate (DIAD) and Ph₃P to generate compound 3. Intermediate 3 was hydrolyzed by NaOH to get compound 4, which was deprotected by sodium thiophenolate

to obtain compound 5. Then, compound 5 was protected by (Boc)₂O to afford the desired intermediate 6.

Peptides (Table 1) were synthesized by manually applying the standard Fmoc methodology by 2-chlorotrityl chloride resin and Fmoc-protected amino acids, as we reported before.²⁶ The synthesized peptides were purified by semi-preparative reversed-phase high-performance liquid chromatography (RP-HPLC). The identification and purity of the final compounds were verified using high-resolution mass spectrometry (HRMS), nuclear magnetic resonance (NMR), and analytical HPLC (see the Supporting Information).

2.2. Biological Activity. **2.2.1. Development and Optimization FP-Based Competitive Assay.** To test the binding affinities between the designed peptides and the nNOS PDZ domain, FP assay was performed. The GST fusion protein of the N-terminal 1–133 of nNOS PDZ domain was utilized as the FP assay protein. GST-tagged nNOS_{1–133} was prepared from *E. coli* 21(DE3) strain as described in the experimental section. The C-terminal amino acid (496–506) sequence of CAPON is LGDGLDDEIAV.¹⁷ We designed a fluorescence probe 5-FAM labeled CAPON (496–506) peptide, 5-FAM-KV-14 (5-FAM-KSGLGDGLDDEIAV), which can be used for FP-based assay. The peptide was synthesized by Fmoc-solid phase peptide synthesis with 2-chlorotrityl chloride resin. 5-Fam was coupled to CAPON terminal 11 peptide by a tripeptide spacer (KSG) with HATU reagent.^{19,21} After removing the protective group, 5-FAM labeled peptide was cleaved from the resin by treatment with TFA, precipitated with ice ether, filtered, dried, and purified by preparative HPLC. The identification and purity of 5-FAM-KV-14 was verified using MS and analytical HPLC (Figure S1).

Initially, to determine of the optimal concentration of the free probe (5-FAM-KV-14) for the FP assay, the experiment was performed by varying 18 concentrations of the free probe from 0.1 to 1000 nM. As shown in Figure 1A, with the 5-FAM-KV-14 concentration increasing, the FP value decreased rapidly and finally reached a stable level. We chose a low concentration (50 nM) of 5-FAM-KV-14, which could yield a stable FP value and reasonable fluorescent signal.

To determine the optimal concentration of GST-tagged nNOS_{1–133}, we evaluated 18 different concentrations of the GST-tagged nNOS_{1–133}, which varied from 1 nM to 20 μ M using a fixed probe concentration of 50 nM. As presented in Figure 1B, with the protein concentration increasing, the FP values showed an s-curve change, which conforms to the general rule of intermolecular interaction. The concentration corresponding to 80% of the maximum FP value was the optimal protein concentration. So, we chose 1 μ M as the optimal protein concentration. When the protein concentration was 1 μ M, the range of the FP value changed the most significantly. This concentration point made the assay sensitive, and the consumption of protein was also relatively economical.

To evaluate the effect of incubation time, the binding experiments were performed using 50 nM 5-FAM-KV-14 with increasing concentrations of GST-nNOS_{1–133} protein (from 1 nM to 20 μ M). The plates were measured at 1, 2, 4, 8, and 24 h, and the results are shown in Figure 1C. After incubation for 1, 2, 4, 8, and 24 h, the FP values remained basically unchanged and stable. The change of the K_d values was very slight (1 h K_d = 0.30 μ M, 2 h K_d = 0.35 μ M, 4 h K_d = 0.31 μ M, 8 h K_d = 0.31 μ M, and 24 h K_d = 0.31 μ M). Therefore, given

the above result and saving time, the incubation time for the binding experiment was chosen as 1 h.

We also explored the influence of dimethyl sulfoxide (DMSO) on the FP assay, which was a commonly used solvent for dissolving some insoluble compounds in the high-throughput screening. The data showed that the binding affinity of 5-FAM-KV-14 was unchanged and the FP assay performed well in the presence of up to 12% DMSO (Figure 1D).

To identify the reliability and quality of the FP assay for the high-throughput screening, the assay performance parameters Z' factor and signal-to-noise (S/N) ratio were determined. The FP assay resulted in an excellent S/N (140.9) ratio and Z' factor value (0.96). Therefore, it was confirmed that the FP assay conditions were adequate for high-throughput screening of blockers for GST-nNOS_{1–133} with 5-FAM-KV-14 as the probe.

In conclusion, a FP-based assay to evaluate the binding affinity of small-molecule blockers that target the nNOS PDZ domain was developed and verified. The assays using 5-FAM-KV-14 as the probe and GST-nNOS_{1–133} as the protein were stable with up to 12% DMSO and 1–24 h incubation time and had a Z' factor value of 0.96, making it suitable for high-throughput screening.

2.2.2. Binding Affinity Evaluated with FP Assay. To evaluate the binding affinities between our designed peptides and the nNOS PDZ, the FP assay was performed as described. All IC₅₀ and K_i values reported in the present study were obtained from at least three independent experiments. The preliminary and secondary screening results are summarized in Table 1 and Figures 2 and 3. Compounds Che-ADWV, Che-ADAV, Che-ADIV, Che-GDLV, and Che-GDWV showed preferable inhibitory rates (>86%, Table 1) with a concentration of 1 mM. Compounds Che-AEAV, Che-AEWV, Che-GDAV, Che-GDPV, and Che-GDFV also displayed moderate potencies (>65%). However, Che-AEFV and Che-AEIV (<13%) showed poor competitive binding activities compared

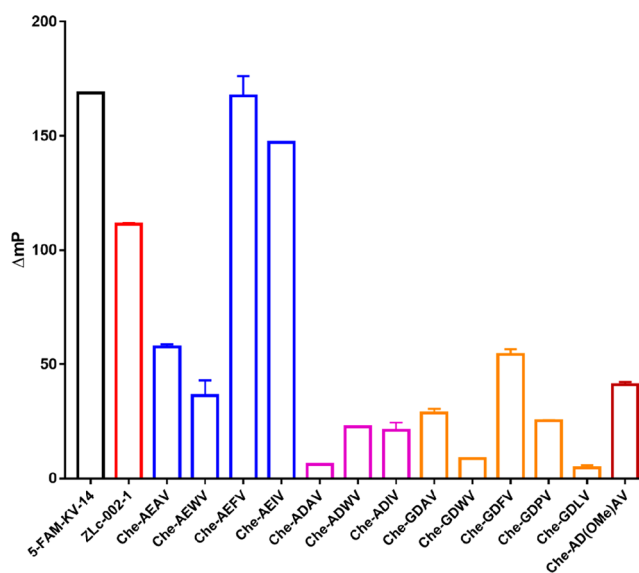


Figure 2. Preliminary FP screening results of designed compounds and reference compounds ZLc-002-1 (a nNOS–CAPON interaction blocker). The assay was performed with 50 nM 5-FAM-KV-14, 1 μ M GST-nNOS_{1–133} protein, 1 h incubation time, and 5% DMSO. The concentration of the tested compounds was 1 mM.

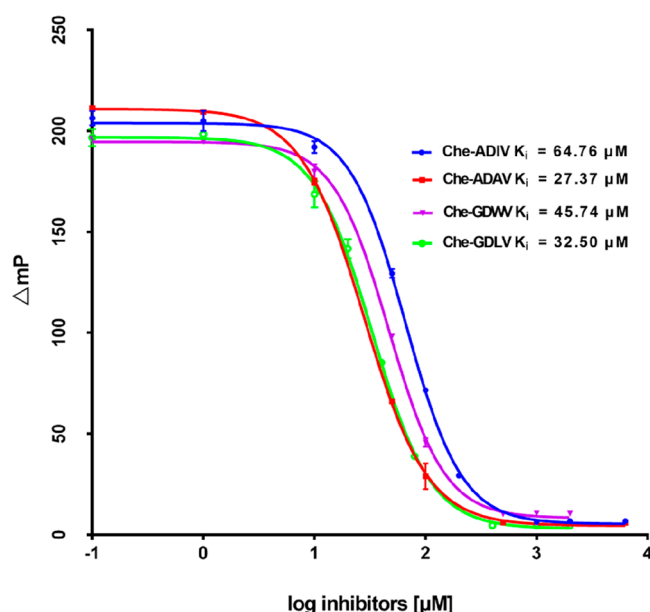


Figure 3. Secondary FP screening results of Che-ADIV, Che-ADAV, Che-GDWV, and Che-GDLV. The assay was performed with 50 nM 5-FAM-KV-14, 1 μ M GST-nNOS_{1–133} protein, 1 h incubation time, and 5% DMSO.

with 5-FAM-KV-14 to the GST-nNOS_{1–133}. Those compounds with high affinities were picked out for the secondary screening. Furthermore, comparing the affinities of compounds Che-AEAV (inhibition ratio = 65.87%) and Che-ADAV (inhibition ratio = 96.38%, K_i = 27.37 μ M), we observed that the Asp improved the affinity more than Glu in the P^{2–} position. A similar effect was observed when comparing Che-AEIV (inhibition ratio = 12.79%) and Che-ADIV (inhibition ratio = 87.44%) or Che-AEWV (inhibition ratio = 78.45%) and Che-ADWV (inhibition ratio = 96.06%, K_i = 73.15 μ M). The -COOH in the side chain of Asp could probably more easily form H-bond interactions with the phenolic hydroxyl of Tyr71 or guanidino of Arg79 of the nNOS PDZ domain. In the P^{3–} position, the substitution of Ala with Gly did not affect the binding potency significantly, as in Che-ADAV (inhibition ratio = 96.38%, K_i = 27.37 μ M) and Che-GDAV (inhibition ratio = 82.99%) or Che-ADWV (inhibition ratio = 86.61%, K_i = 73.15 μ M) and Che-GDWV (inhibition ratio = 94.84%, K_i = 45.74 μ M), demonstrating that lipophilic amino acids in the P^{3–} position had a lower effect on the overall activity of the compounds. At the P^{1–} position, it accommodated several amino acids, such as Trp, Ala, Ile, Pro, and Leu, however, Phe was hardly bound into the nNOS PDZ domain as shown in Che-GDFV and Che-AEFV. Although further investigation on the SAR was needed, these findings could provide more experience for the further optimization of nNOS–CAPON interaction blockers.

2.2.3. ITC Assay. Isothermal titration calorimetry (ITC) was used to fit the binding process of 5-FAM-KV-14 and GST-nNOS_{1–133} protein to verify that the binding was a typical single-point binding. (Figure 4A). The titration results of Che-AEAV and Che-ADAV to GST-nNOS_{1–133} are shown in Figure 4. The thermodynamic parameters of the binding of the designed peptides to the nNOS PDZ domain obtained by ITC are summarized in Table 2. Che-ADAV exhibited a high affinity to GST-nNOS_{1–133} (ΔH = -1670 ± 151.0 cal/mol). The results of the ITC screening correlated well with the FP

experiment, also indicating that FP could be used as a screening method for nNOS–CAPON binding blockers.

2.2.4. Molecule Docking Study. In order to explore the binding mode between Che-ADAV and nNOS PDZ, we performed a semiflexible molecular docking between Che-ADAV and the nNOS PDZ domain (PDB code: 1B8Q) using Discovery Studio 3.5. The interaction energy was -61.73 kcal/mol. As shown in Figure 5, Che-ADAV was tightly bound into the groove between the α B helix and β B folding of the nNOS PDZ domain. In the Che-ADAV–nNOS PDZ domain complex, there were hydrogen-bonding interactions between the Che-ADAV and GLGF loop (Gly21–Leu22–Gly23–Phe24) of the nNOS PDZ domain. The -COOH of Val (Che-ADAV) formed a H-bond with Gly23; the hydrogen-bond distance was 2.03 Å. The Asp (Che-ADAV) made double H-bonds with Tyr71 and Arg79, respectively, and the H-bond distances were 2.07 and 2.04 Å, respectively. In addition, the Ala (Che-ADAV) interacted with Val26 using a H-bond.

2.2.5. Structure Optimization of Che-ADAV and in Vitro PAMPA-BBB Assay of Che-ADAV and Che-AD(OMe)AV. To improve bioavailability, lipophilicity, and membrane permeability, the Asp methylation of Che-ADAV was employed to get Che-AD(OMe)AV. Compounds Che-AD(OMe)AV and Che-ADAV were assayed in the FP binding experiment (Figure 2). Che-ADAV displayed more potent binding affinity with the nNOS PDZ domain than did Che-AD(OMe)AV. As shown in Figure 4D and Table 2, these two compounds were also compared by the ITC assay to further confirm the binding affinity with nNOS PDZ domain. Che-AD(OMe)AV (ΔH = -967.7 ± 312.4 cal/mol) exhibited a weaker affinity to GST-nNOS_{1–133} compared with Che-ADAV (ΔH = -1670 ± 151.0 cal/mol). The data indicated that the conversion of the Asp carboxylate to an ester greatly reduced the binding affinity because the salt bridge/electrostatic interaction with Arg79 would be eliminated and H-bond interactions would be reduced. To verify and compare the BBB permeability of compounds Che-ADAV and Che-AD(OMe)AV, we carried out the parallel artificial membrane permeability assay of BBB (PAMPA-BBB) (Figure 6). The result showed that compound Che-AD(OMe)AV (P_e = 6.07 cm/s) displayed a much higher permeability value than Che-ADAV (P_e = 2.65 cm/s), which suggested that compound Che-AD(OMe)AV could more easily penetrate into the BBB than Che-ADAV.

2.2.6. In Vivo Brain Pharmacokinetic Study. To evaluate the permeability across the BBB *in vivo* of compound Che-AD(OMe)AV and whether it was converted to Che-ADAV or not, we measured the concentrations of Che-AD(OMe)AV and Che-ADAV in brain tissue at 1 min, 5 min, 30 min, 45 min, 1 h, and 2 h after intraperitoneal injection (20 mg/kg). As shown in Table 3, the precursor ion of Che-AD(OMe)AV was 499.3 and the product ion was 154.3. The precursor ion of Che-ADAV was 485.3 and the product ion was 154.3. Fluoxetine was used as an internal reference (the precursor ion of fluoxetine was 310.2 and the product ion was 148.1). *In vivo* brain pharmacokinetic studies indicated that Che-AD(OMe)AV displayed a good brain uptake (136.7 ng/g at 45 min). Che-AD(OMe)AV was acting as a prodrug and was converted to the active carboxylate form Che-ADAV. The concentration of Che-ADAV reached the high pot in brain tissue at about 45 min after administration (Figure 7). Detailed data can be found in the Supporting Information.

2.2.7. Che-AD(OMe)AV Attenuated Nerve Injury of MCAO Rats. Having confirmed the effective blood–brain barrier

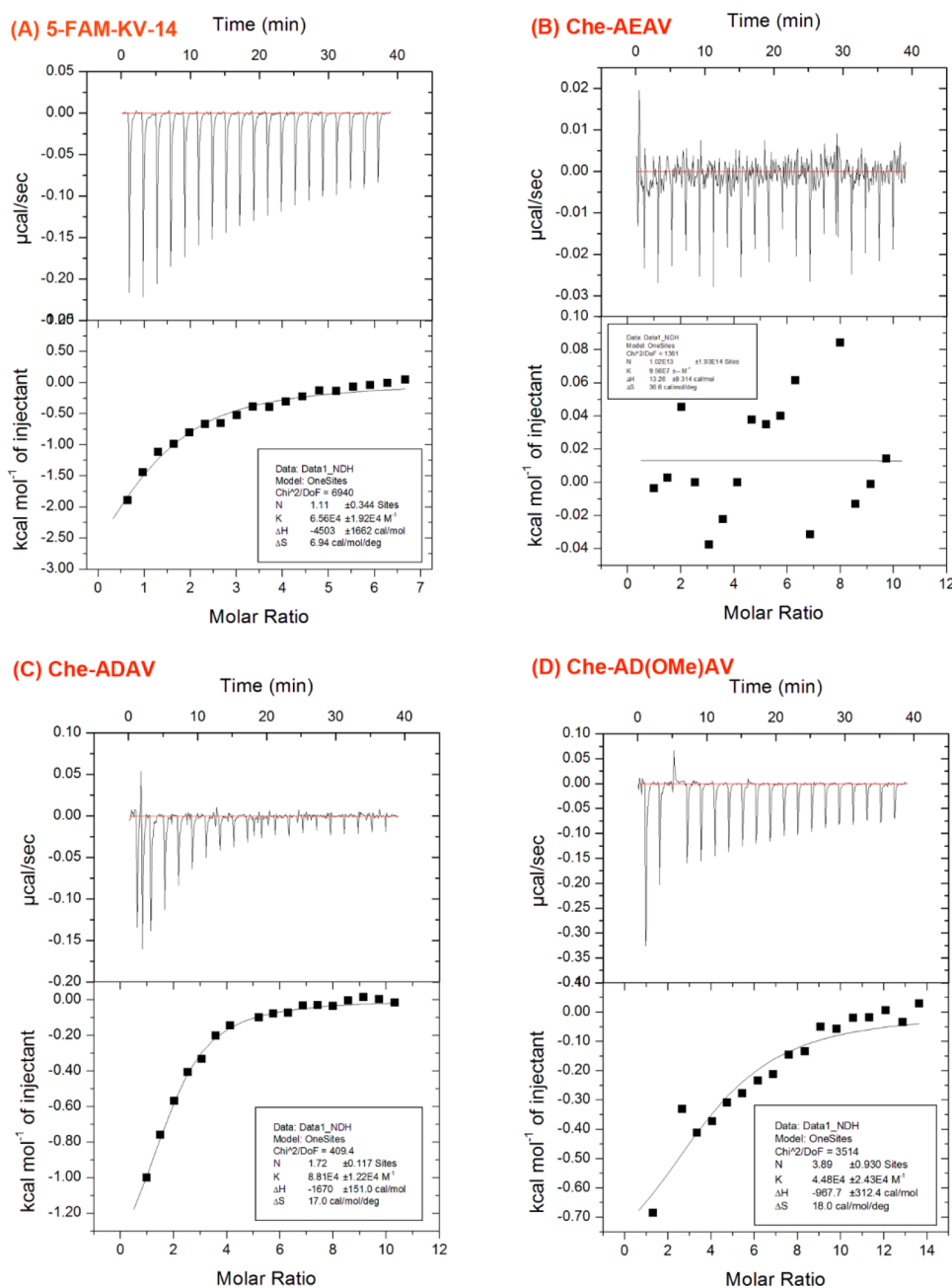


Figure 4. ITC data for binding of (A) 5-FAM-KV-14, (B) Che-AEAV, (C) Che-ADAV, and (D) Che-AD(OMe)AV GST-nNOS₁₋₁₃₃. The upper panel of the graph shows the heat flow of each injection; the lower panel indicates the integration of each peak (kcal/mol) as a function of the molar ratio of compounds to GST-nNOS₁₋₁₃₃ after subtracting the heat of dilution. The thermodynamic parameters (K , ΔH , and ΔS) are indicated in the picture.

Table 2. Thermodynamic Parameters of the Binding of the Designed Peptides to the nNOS PDZ Domain Obtained by ITC

compounds	N	K (M^{-1})	ΔH (cal/mol)	ΔS (cal/mol/deg)
5-FAM-KV-14	1.11	$6.56 \times 10^4 \pm 1.92 \times 10^4$	-4503 ± 1662	6.94
Che-AEAV	1.02×10^{13}	9.56×10^7	$+13.26 \pm 9.314$	36.6
Che-ADAV	1.72	$8.81 \times 10^4 \pm 1.22 \times 10^4$	-1670 ± 151.0	17.0
Che-AD(OMe)AV	3.89	$4.48 \times 10^4 \pm 2.43 \times 10^4$	-967.7 ± 312.4	18.0

permeability of compound Che-AD(OMe)AV, we next moved on to investigate its neuroprotective ability *in vivo* by a middle cerebral artery occlusion (MCAO) model that was widely used for the ischemic stroke study. Infarct size was measured following sacrifice at 24 h by staining of 1 mm thick brain slices with 2,3,5-triphenylterazolium hydrochloride (TTC). We used

edaravone as the positive drug for its superior neuroprotective ability described in previous reports.¹ As shown in Figure 8, a white region of the brain sections (23.9, vehicle) indicated an infarction that was induced by MCAO. Treatment with 10 mg/kg compound Che-AD(OMe)AV significantly reduced the ischemia area to 4.8% ($p < 0.001$ vs vehicle). As a comparison,

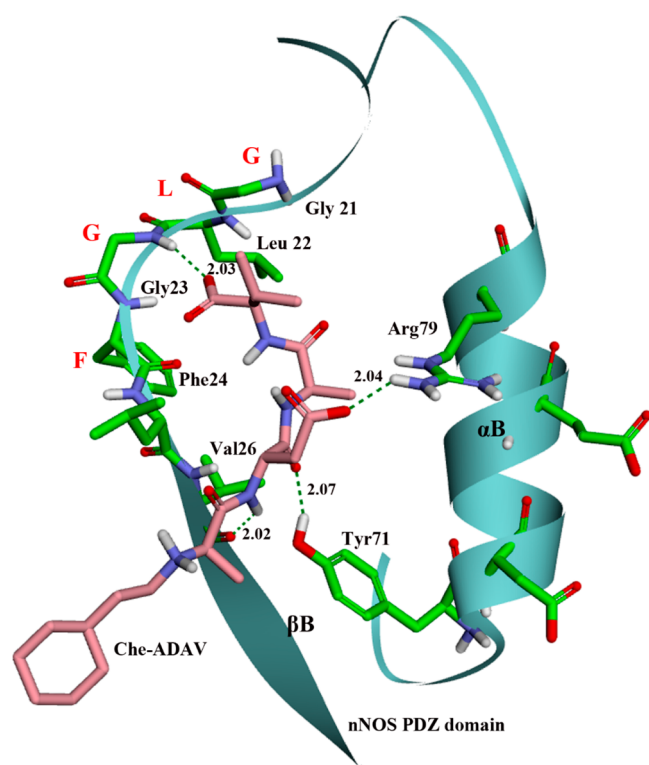


Figure 5. Interaction of Che-ADAV with the nNOS PDZ domain.

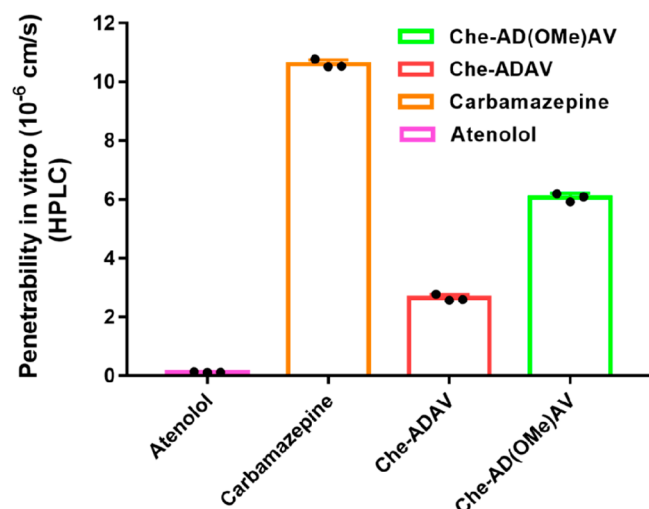


Figure 6. Ratio of penetrability *in vitro* of compounds in the PAMPA-BBB assay was carried out and calculated by HPLC after an incubation of 18 h. Carbamazepine (high brain penetration) was selected as the positive control, and atenolol (low brain penetration) was selected as the negative control. Data were shown as mean \pm SEM of three independent experiments.

Table 3. Mass Parameters for the Detection of Che-AD(OMe)AV and Its Metabolite Che-ADAV

compounds	precursor ion	product ion	fragmentor	collision energy
Che-AD(OMe)AV	499.3	154.3	145	30
Che-ADAV	485.3	154.3	145	30
Fluoxetine	310.2	148.1	105	4

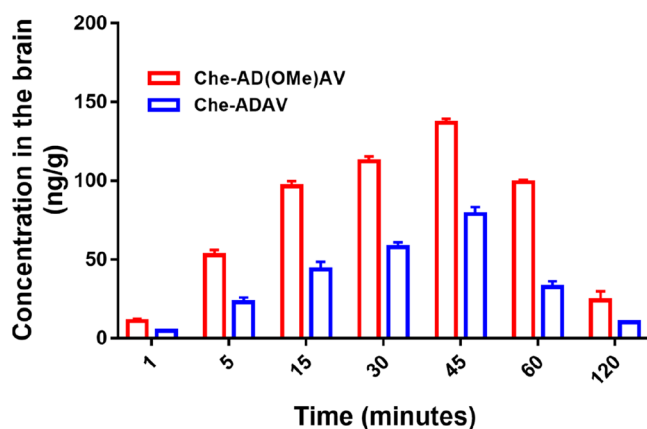


Figure 7. Concentrations of Che-AD(OMe)AV and Che-ADAV: time column chart of mice brain tissue after intraperitoneal injection (20 mg/kg) for 1 min, 5 min, 30 min, 45 min, 1 h, and 2 h.



Figure 8. Representative of triphenyltetrazolium chloride stained brain slices.

the edaravone group reduced the ischemia area to 9.2% ($p < 0.01$ vs vehicle). The compound Che-AD(OMe)AV decreased the ischemia area by 4.4% compared with the edaravone group (Figure 9). These results suggested that the compound Che-AD(OMe)AV could be a potential neuroprotective compound against cerebral ischemia damage.

3. CONCLUSION

In summary, we designed and synthesized a series of Che-[A/G]-[D/E]-X-V peptides based on the carboxy-terminal tetrapeptide of CAPON that is capable of blocking nNOS-CAPON coupling. Herein, we reported an affinity-based FP

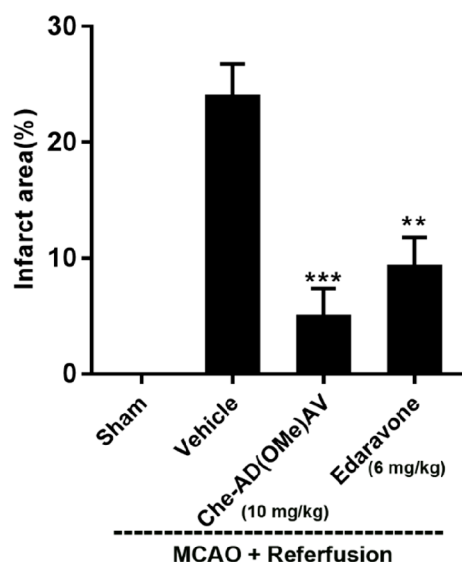


Figure 9. Effects of Che-AD(OMe)AV and positive compound edaravone on cerebral ischemia in rats subjected to 120 min MCAO. Infarct size was measured at 24 h after reperfusion. ($n = 16$ – 18 , data are presented as mean \pm SEM, $^{***}P < 0.01$, $^{***}P < 0.001$, vs vehicle-treated MCAO group, one-way ANOVA, followed by *post hoc* Scheffe test).

method using 5-FAM-KSGLGDLDDLEIAV as a probe for high-throughput screening of the binding affinities of our designed peptides with the PDZ domain of nNOS. The most potent peptide (Che-ADAV) binds to nNOS PDZ with a K_i value of $27.37 \mu\text{M}$ in the FP assay. The ITC was employed to confirm the binding activity between Che-ADAV to GST-nNOS_{1–133}. Che-ADAV exhibited a high affinity to GST-nNOS_{1–133} ($\Delta H = -1670 \pm 151.0 \text{ cal/mol}$). The results of ITC screening correlated well with the FP experiment. To improve bioavailability, lipophilicity, and membrane permeability, the Asp methylation was employed to get Che-AD(OMe)AV, which possesses good BBB permeability *in vitro* PAMPA-BBB ($P_e = 6.07 \text{ cm/s}$) and *in vivo* assays. In addition, Che-AD(OMe)AV (10 mg/kg body weight, *i.v.*, after reperfusion) substantially reduced the infarct size in rats subjected to 120 min of MCAO.

4. MATERIALS AND METHODS

4.1. Chemistry. **4.1.1. RP-HPLC was Performed on a Waters Delta 600 Liquid Chromatograph Using the Following Solvent System.** Solvent A, 0.05% TFA in water; solvent B, 0.05% TFA in CH_3CN . Semipreparative RP-HPLC was performed on a Sunfire Prep C18 column (20 mm \times 250 mm) with a linear gradient of 5–50% of solvent B over 40 min at a flow rate of 10 mL/min. Analytical RP-HPLC was performed on a Sunfire Prep C18 column (4.6 mm \times 250 mm) with a linear gradient of 5–50% of solvent B over 40 min at a flow rate of 1.2 mL/min. ^1H and ^{13}C NMR spectra were recorded on a JEOL 400 MHz spectrometer at 25°C .

4.1.2. Synthesis of *N*-(2-Nitrobenzenesulfonyl)-*L*-alanine Methyl Ester (2). To a solution of *L*-alanine methyl ester (6 g, 58.2 mmol, 1 equiv) in DCM (100 mL) was added 2-nitrobenzenesulfonyl chloride (12.9 g, 58.2 mmol, 1 equiv) and triethylamine (16 mL, 116.4 mmol, 2 equiv) at 0°C . The mixture was stirred at room temperature for 2 h and then washed with water. The organic layer was separated and dried with Na_2SO_4 and concentrated. The brown solid was purified by column chromatography to give desired compound 2 at 15 g. Yield: 89%. ^1H NMR (400 MHz, $\text{DMSO}-d_6$): δ 8.73 (s, 1H), 8.04–7.92 (m, 2H), 7.89–7.82 (m, 2H), 4.06 (q, $J = 7.1 \text{ Hz}$, 1H), 3.46 (s, 3H), 1.28 (d, $J = 7.2 \text{ Hz}$, 3H). MS (ESI, m/z): 311.0 $[\text{M} + \text{Na}]^+$.

4.1.3. Synthesis of *N*-(2-Cyclohexylethyl)-*N*-((2-nitrophenyl)-sulfonyl) Alanine Methyl Ester (3). To a cold mixture of compound 2 (15 g, 52 mmol), triphenylphosphine (20.46 g, 78 mmol 1.5 equiv), and 2-cyclohexylethan-1-ol (7.25 mL, 52 mmol, 1 equiv) in 500 mL of dry THF and under a N_2 atmosphere was slowly added diisopropyl azodiformate (DIAD, 15.76 g, 78 mmol, 1.5 equiv), and the mixture was stirred overnight at room temperature. The solvent was evaporated, and the residue was extracted with EtOAc (200 mL \times 3). The EtOAc layers were combined, washed with brine, dried with Na_2SO_4 , and concentrated. The crude product was chromatographed on silica to obtain 15.1 g of the expected compound 3. Yield: 73%. ^1H NMR (400 MHz, CDCl_3): δ 8.16–7.97 (m, 1H), 7.72 (m, 2H), 7.65–7.55 (m, 1H), 4.75 (q, $J = 7.3 \text{ Hz}$, 1H), 3.59 (s, 3H), 3.53–3.04 (m, 2H), 1.68–0.82 (m, 16H).

4.1.4. Synthesis of *N*-(2-Cyclohexylethyl)-*N*-((2-nitrophenyl)-sulfonyl) Alanine (4). Compound 3 (15 g, 37.6 mmol) and 1 N NaOH (45 mL, 45 mmol) were dissolved in MeOH (50 mL). The mixture was reacted overnight at room temperature. After the reaction, the residue was dissolved in water, acidified to pH 1–2 with 2 N HCl, and extracted with EtOAc (150 mL \times 3). The organic phases were combined, washed with a saturated aqueous solution of NaCl, and dried and evaporated to dryness to afford a yellow oil. The yellow oil was purified by silica gel column chromatography ($\text{CH}_2\text{Cl}_2/\text{MeOH} = 20:1$) to give intermediate compound 4 at 13.5 g. Yield: 93%. ^1H NMR (400 MHz, CDCl_3): δ 9.75 (s, 1H), 8.18–7.98 (m, 1H), 7.71 (m, 2H), 7.64 (m, 1H), 4.78 (q, $J = 7.3 \text{ Hz}$, 1H), 3.58–3.00 (m, 2H), 1.99–0.79 (m, 16H). MS (ESI, m/z): 407.1 $[\text{M} + \text{Na}]^+$.

4.1.5. Synthesis of *N*-(*tert*-Butoxycarbonyl)-*N*-(2-cyclohexylethyl) Alanine (6). To a solution of compound 4 (13 g, 34 mmol) in dry DMF (50 mL) was added sodium thiophenolate (9 g, 68 mmol), and then, the mixture was stirred overnight at room temperature. The mixture was concentrated under reduced pressure. Water was added to dissolve the crude mixture. The solution was acidified to pH 4 with 2 N HCl and extracted with ether three times. The aqueous layers were collected, pH adjusted to 5–6, and freeze-dried to achieve a pale-yellow solid, which could be used in the next reaction without further purification. MS (ESI, m/z): 222.1 $[\text{M} + \text{Na}]^+$.

To compound 5 and triethylamine (19 mL, 136 mmol) in 1,4-dioxane was added $(\text{Boc})_2\text{O}$ (22.3 g, 102 mmol) at room temperature. After stirring overnight, the residue was concentrated, and then taken up in water as the solvent and pH adjusted to 3–4 by 10% citric acid. The mixture was extracted with ethyl acetate three times. The organic phase was dried, evaporated to dryness, and purified by silica gel column chromatography ($\text{CH}_2\text{Cl}_2/\text{MeOH} = 20:1$) to get compound 6 at 5.1 g. Yield: 50%. ^1H NMR (400 MHz, CDCl_3): δ 11.31 (s, 1H), 4.42–3.99 (m, 1H), 3.36–3.06 (m, 2H), 1.81–0.84 (m, 26H). MS (ESI, m/z): 322.2 $[\text{M} + \text{Na}]^+$.

4.1.6. General Procedure for the Fmoc Solid-Phase Synthesis. Peptides were synthesized by manual applying the standard Fmoc methodology. 2-Chlorotrityl chloride resin (100–200 mesh, 0.3–0.8 mmol/g, 1% DVB) and Fmoc-protected amino acids (Fmoc-Val-OH, Fmoc-Ala-OH, Fmoc-Trp(Boc)-OH, Fmoc-Phe-OH, Fmoc-Ile-OH, Fmoc-Pro-OH, Fmoc-Leu-OH, Fmoc-Glu(*t*Bu)-OH, Fmoc-Asp(*t*Bu)-OH, and Fmoc-Gly-OH) were purchased from GL Biochem Ltd. (Shanghai, China). The coupling reagents HBTU, HOBt, and DIPEA were also purchased from GL Biochem Ltd. (Shanghai, China). Dichloromethane (DCM), *N,N*-dimethylformamide (DMF), tetrahydrofuran (THF), piperidine, and other solvents were redistilled and stored with molecular sieves. All reagents and chemicals were ACS grade or better and were used without further purification. The growing peptide chain was added to the swelled 2-chlorotrityl chloride resin using the general amino acid cycle as follows: (1) the addition of Fmoc-amino acid (4 equiv), HBTU (4 equiv), DIPEA (4 equiv), and HOBt (4 equiv) in dry DMF, mixing and shaking for 4 h at 25°C ; (2) monitoring the completion of the reaction with the ninhydrin test; (3) filtering and washing with DMF (15 \times 3 mL) to totally take off the unreacted Fmoc amino acid; (4) deprotecting the Fmoc group with 20% (v/v) piperidine in DMF (10 min) and Fmoc deprotection one more time (30 min); (5) monitoring the completion of the reaction with the ninhydrin test; (6) washing with DMF (10 mL \times 3).

After a complete peptide assembly, the resin was washed with DMF (3 × 5 mL) and CH₂Cl₂ (3 × 5 mL) and was dried in a desiccator overnight. Peptides were cleaved from the resin by treatment with TFA/tips (19/1, 10 mL of the mixture/g of resin) for 2 h at 25 °C, and the cleavage procedure was repeated twice. The crude product was analyzed by HPLC and was purified by semipreparative RP-HPLC. The HPLC analysis column was a Sunfire Prep C18 column (4.6 mm × 250 mm), and the semipreparation column was a Sunfire Prep C18 column (20 mm × 250 mm). After semipreparation, the product peak was collected and freeze-dried to obtain the desired peptide.

4.1.6.1. N-Cyclohexylethyl-Ala-Glu-Ala-Val-OH (Che-AEAV). Yield 155.5 mg (15.61%). HPLC: t_R = 13.45 min. ¹H NMR (300 MHz, DMSO-*d*₆): δ 12.30 (s, 2H), 8.64 (d, *J* = 8.3 Hz, 1H), 8.07 (d, *J* = 7.1 Hz, 1H), 7.90 (d, *J* = 8.6 Hz, 1H), 4.34 (t, *J* = 7.0 Hz, 2H), 4.10 (dd, *J* = 8.5, 5.7 Hz, 1H), 3.89 (s, 1H), 2.78 (s, 3H), 2.24 (t, *J* = 8.0 Hz, 2H), 2.01–1.89 (m, 1H), 1.87 (d, *J* = 5.2 Hz, 1H), 1.83–1.68 (m, 1H), 1.61–1.47 (m, 5H), 1.42 (t, *J* = 7.6 Hz, 2H), 1.33 (d, *J* = 6.8 Hz, 3H), 1.18 (d, *J* = 7.0 Hz, 6H), 0.84 (d, *J* = 6.8 Hz, 9H). HRMS (ESI): *m/z* calcd for C₂₄H₄₃N₄O₇ (M + H)⁺, 499.3132; found, 499.3142.

4.1.6.2. N-Cyclohexylethyl-Ala-Glu-Trp-Val-OH (Che-AEWW). Yield 76.3 mg (12.45%). HPLC: t_R = 14.15 min. ¹H NMR (300 MHz, DMSO-*d*₆): δ 13.04–11.60 (m, 2H), 10.75 (s, 1H), 8.58 (d, *J* = 8.5 Hz, 1H), 8.08 (t, *J* = 8.5 Hz, 2H), 7.82–6.38 (m, 5H), 4.65 (d, *J* = 4.9 Hz, 1H), 4.33 (d, *J* = 5.4 Hz, 1H), 4.21–4.06 (m, 1H), 3.81 (d, *J* = 7.0 Hz, 1H), 3.09 (d, *J* = 10.0 Hz, 2H), 2.97–2.63 (m, 3H), 2.15–2.05 (m, 3H), 2.06 (s, 1H), 1.87 (s, 1H), 1.73 (d, *J* = 7.9 Hz, 1H), 1.60 (d, *J* = 9.5 Hz, 5H), 1.55–1.32 (m, 3H), 1.23–1.12 (m, 4H), 1.13 (s, 3H), 0.87–0.71 (m, 6H). HRMS (ESI): *m/z* calcd for C₃₂H₄₇N₅O₇ (M + H)⁺, 614.3554; found, 614.3556.

4.1.6.3. N-Cyclohexylethyl-Ala-Asp-Trp-Val-OH (Che-ADWW). Yield 38.4 mg (6.41%). HPLC: t_R = 14.35 min. ¹H NMR (300 MHz, DMSO-*d*₆): δ 10.75 (s, 2H), 8.66 (s, 1H), 7.96 (s, 2H), 7.55 (d, *J* = 7.8 Hz, 1H), 7.28 (d, *J* = 8.4 Hz, 1H), 7.13–6.77 (m, 4H), 4.58 (s, 2H), 4.12 (s, 1H), 3.68 (s, 1H), 3.08 (s, 2H), 2.93 (s, 2H), 2.67–2.35 (m, 3H), 2.01 (s, 1H), 1.58 (s, 5H), 1.38 (d, *J* = 7.5 Hz, 3H), 1.23 (d, *J* = 6.8 Hz, 5H), 1.12–0.99 (m, 3H), 0.84 (d, *J* = 4.1 Hz, 6H). HRMS (ESI): *m/z* calcd for C₃₁H₄₅N₅O₇ (M + H)⁺, 600.3397; found, 600.3393.

4.1.6.4. N-Cyclohexylethyl-Ala-Glu-Phe-Val-OH (Che-AEFV). Yield 97.8 mg (17.03%). HPLC: t_R = 10.17 min. ¹H NMR (300 MHz, DMSO-*d*₆): δ 8.56 (d, *J* = 8.0 Hz, 1H), 8.12–8.00 (m, 2H), 7.26–7.07 (m, 5H), 4.62 (s, 1H), 4.29 (d, *J* = 5.2 Hz, 1H), 4.12 (d, *J* = 8.4 Hz, 1H), 3.80 (d, *J* = 7.2 Hz, 1H), 2.99–2.90 (m, 2H), 2.85–2.65 (m, 3H), 2.16 (t, *J* = 8.0 Hz, 2H), 2.03–1.89 (m, 2H), 1.83 (s, 1H), 1.77–1.44 (m, 7H), 1.42–1.17 (m, 6H), 1.13 (s, 3H), 0.89–0.80 (m, 6H). HRMS (ESI): *m/z* calcd for C₃₀H₄₆N₄O₇ (M + H)⁺, 575.3445; found, 575.3450.

4.1.6.5. N-Cyclohexylethyl-Ala-Asp-Ala-Val (Che-ADAV). Yield 33.2 mg (6.86%). HPLC: t_R = 11.18 min. ¹H NMR (300 MHz, DMSO-*d*₆): δ 12.47 (s, 2H), 9.09–8.73 (m, 1H), 7.99 (d, *J* = 6.9 Hz, 1H), 7.90 (s, 1H), 4.63 (s, 1H), 4.44–4.27 (m, 1H), 4.22–4.03 (m, 1H), 3.81 (s, 1H), 2.80 (s, 2H), 2.73–2.50 (m, 2H), 2.52 (d, *J* = 9.6 Hz, 1H), 2.10–1.94 (m, 1H), 1.63–1.42 (m, 5H), 1.44 (d, *J* = 6.7 Hz, 2H), 1.36 (d, *J* = 6.8 Hz, 3H), 1.19 (d, *J* = 7.0 Hz, 6H), 0.87 (s, 3H), 0.85 (s, 6H). HRMS (ESI): *m/z* calcd for C₂₃H₄₀N₄O₇ (M + H)⁺, 485.2975; found, 485.3009.

4.1.6.6. N-Cyclohexylethyl-Ala-Glu-Ile-Val-OH (Che-AEIV). Yield 23.5 mg (4.35%). HPLC: t_R = 12.95 min. ¹H NMR (300 MHz, DMSO-*d*₆): δ 8.54 (s, 1H), 7.92 (d, *J* = 8.5 Hz, 1H), 7.85 (s, 1H), 4.40 (s, 1H), 4.33–4.21 (m, 1H), 4.14–4.05 (m, 1H), 3.73 (s, 1H), 2.75–2.27 (m, 3H), 2.20 (d, *J* = 7.5 Hz, 3H), 2.13–1.96 (m, 2H), 1.88 (s, 1H), 1.74 (s, 2H), 1.63–1.51 (m, 5H), 1.50–1.36 (m, 4H), 1.35–1.10 (m, 7H), 0.87 (d, *J* = 2.7 Hz, 3H), 0.83 (d, *J* = 7.3 Hz, 6H), 0.78 (d, *J* = 7.4 Hz, 3H). HRMS (ESI): *m/z* calcd for C₂₇H₄₈N₄O₇ (M + H)⁺, 541.3601; found, 541.3601.

4.1.6.7. N-Cyclohexylethyl-Ala-Asp-Ile-Val-OH (Che-ADIV). Yield 67.5 mg (12.82%). HPLC: t_R = 10.90 min. ¹H NMR (300 MHz, DMSO-*d*₆): δ 8.75 (d, *J* = 7.9 Hz, 1H), 7.94 (d, *J* = 8.3 Hz, 1H), 7.71 (d, *J* = 9.3 Hz, 1H), 4.65 (d, *J* = 4.8 Hz, 1H), 4.33–4.21 (m, 1H),

4.14–4.02 (m, 1H), 3.71 (d, *J* = 6.7 Hz, 1H), 2.73–2.61 (m, 3H), 2.66 (d, *J* = 4.5 Hz, 1H), 2.52–2.37 (m, 2H), 2.03–1.87 (m, 1H), 1.63–1.50 (m, 6H), 1.48–1.35 (m, 3H), 1.31 (d, *J* = 6.7 Hz, 4H), 1.17–0.98 (m, 3H), 0.91 (s, 2H), 0.87 (d, *J* = 2.5 Hz, 3H), 0.84 (d, *J* = 4.9 Hz, 6H), 0.77 (d, *J* = 7.4 Hz, 3H). HRMS (ESI): *m/z* calcd for C₂₆H₄₆N₄O₇ (M + H)⁺, 527.3445; found, 527.3446.

4.1.6.8. N-Cyclohexylethyl-Gly-Asp-Ala-Val-OH (Che-GDAV). Yield 248.6 mg (26.42%). HPLC: t_R = 16.50 min. ¹H NMR (300 MHz, DMSO-*d*₆): δ 12.59 (s, 2H), 8.73–8.61 (m, 1H), 8.10 (d, *J* = 7.0 Hz, 1H), 7.88–7.72 (m, 1H), 4.69–4.53 (m, 1H), 4.43–4.26 (m, 1H), 4.15–4.04 (m, 1H), 3.70 (s, 2H), 2.98–2.81 (m, 2H), 2.69–2.67 (m, 1H), 2.61–2.50 (m, 2H), 2.04–1.89 (m, 1H), 1.63–1.41 (m, 5H), 1.45–1.23 (m, 2H), 1.19 (t, *J* = 6.3 Hz, 4H), 1.00–0.93 (m, 3H), 0.95 (s, 2H), 0.85 (s, 6H). HRMS (ESI): *m/z* calcd for C₂₂H₃₈N₄O₇ (M + H)⁺, 471.2819; found, 471.2837.

4.1.6.9. N-Cyclohexylethyl-Gly-Asp-Pro-Val-OH (Che-GDPV). Yield 176.3 mg (17.78%). HPLC: t_R = 14.17 min. ¹H NMR (300 MHz, DMSO-*d*₆): δ 12.51 (s, 2H), 8.90 (d, *J* = 7.7 Hz, 1H), 7.81 (d, *J* = 8.5 Hz, 1H), 4.87 (d, *J* = 5.4 Hz, 1H), 4.40 (d, *J* = 6.3 Hz, 1H), 4.12–4.03 (m, 1H), 3.69 (s, 2H), 3.65–3.54 (m, 2H), 2.90 (s, 2H), 2.72–2.66 (m, 1H), 2.50 (s, 2H), 2.47–2.38 (m, 2H), 2.04–1.97 (m, 1H), 1.89 (s, 2H), 1.54–1.31 (m, 7H), 1.30–1.08 (m, 4H), 0.92 (d, *J* = 7.0 Hz, 2H), 0.86 (d, *J* = 6.8 Hz, 6H). HRMS (ESI): *m/z* calcd for C₂₄H₄₀N₄O₇ (M + H)⁺, 497.2975; found, 497.2987.

4.1.6.10. N-Cyclohexylethyl-Gly-Asp-Leu-Val-OH (Che-GDLV). Yield 318 mg (31.06%). HPLC: t_R = 13.90 min. ¹H NMR (300 MHz, DMSO-*d*₆): δ 8.75 (d, *J* = 7.9 Hz, 1H), 8.09 (d, *J* = 8.1 Hz, 1H), 7.80 (d, *J* = 8.4 Hz, 1H), 4.64–4.58 (m, 1H), 4.34–4.27 (m, 1H), 4.13–4.00 (m, 1H), 3.77–3.56 (m, 2H), 2.90 (s, 2H), 2.75–2.58 (m, 1H), 2.50 (d, *J* = 9.5 Hz, 2H), 2.02–1.87 (m, 1H), 1.64 (s, 2H), 1.61 (s, 4H), 1.46–1.38 (m, 4H), 1.28–1.04 (m, 4H), 0.89 (d, *J* = 9.2 Hz, 2H), 0.87–0.78 (m, 12H). HRMS (ESI): *m/z* calcd for C₂₅H₄₄N₄O₇ (M + H)⁺, 513.3288; found, 513.3304.

4.1.6.11. N-Cyclohexylethyl-Gly-Asp-Phe-Val-OH (Che-GDFV). Yield 151.5 mg (13.74%). HPLC: t_R = 14.15 min. ¹H NMR (300 MHz, DMSO-*d*₆): δ 12.62 (s, 2H), 8.69–8.43 (m, 1H), 8.22–7.93 (m, 2H), 7.22–6.89 (m, 5H), 4.72–4.41 (m, 2H), 4.13 (dd, *J* = 8.2, 6.0 Hz, 1H), 3.62–3.54 (m, 2H), 3.43 (s, 2H), 3.08–2.95 (m, 1H), 2.67–2.59 (m, 2H), 2.50–2.36 (m, 2H), 2.05–1.78 (m, 1H), 1.53–1.44 (m, 7H), 1.31–1.00 (m, 4H), 0.94–0.74 (m, 8H). HRMS (ESI): *m/z* calcd for C₂₈H₄₂N₄O₇ (M + H)⁺, 547.3132; found, 547.3251.

4.1.6.12. N-Cyclohexylethyl-Gly-Asp-Trp-Val-OH (Che-GDWW). Yield 189.1 mg (16.16%). HPLC: t_R = 14.10 min. ¹H NMR (300 MHz, DMSO-*d*₆): δ 10.78 (d, *J* = 8.8 Hz, 1H), 8.67–8.57 (m, 1H), 8.16–7.94 (m, 2H), 7.57 (d, *J* = 6.4 Hz, 1H), 7.30 (d, *J* = 7.9 Hz, 1H), 7.13–6.91 (m, 3H), 4.69–4.52 (m, 2H), 4.12 (d, *J* = 8.8 Hz, 1H), 3.70–3.53 (m, 2H), 3.12–3.01 (m, 2H), 2.98–2.80 (m, 3H), 2.76–2.50 (m, 2H), 2.04–1.66 (m, 1H), 1.56–1.44 (m, 6H), 1.42 (s, 1H), 1.27–1.07 (m, 4H), 0.87 (d, *J* = 6.4 Hz, 8H). HRMS (ESI): *m/z* calcd for C₃₀H₄₃N₅O₇ (M + H)⁺, 586.3241; found, 586.3250.

4.1.6.13. N-Cyclohexylethyl-Ala-Asp-OMe-Ala-Val (Che-AD-(OMe)AV-OH). Yield 88 mg (16.7%). HPLC: t_R = 19.85 min. ¹H NMR (400 MHz, DMSO-*d*₆): δ 8.88 (d, *J* = 8.0 Hz, 1H), 8.14 (d, *J* = 8.9 Hz, 1H), 7.89 (d, *J* = 9.6 Hz, 1H), 4.68–4.63 (m, 1H), 4.34–4.27 (m, 1H), 4.11–4.07 (m, 1H), 3.81–3.76 (m, 1H), 3.54 (s, 3H), 2.87–2.72 (m, 3H), 2.55–2.42 (m, 2H), 2.05–1.97 (m, 1H), 1.61–1.54 (m, 5H), 1.44–1.38 (m, 2H), 1.29 (d, *J* = 6.9 Hz, 3H), 1.24–1.05 (m, 7H), 0.83 (d, *J* = 6.7 Hz, 8H). HRMS (ESI): *m/z* calcd for C₂₄H₄₂N₄O₇ (M + H)⁺, 499.3132; found, 499.3137.

4.2. Biological Evaluation. **4.2.1. Expression, Purification and Identification of GST-nNOS PDZ.** *E. coli* 21(DE3) containing pGEX4T-1-GST-nNOS_{1–133} was inoculated into 5 mL of LB medium (1:1000) with 50 μg/mL ampicillin and cultured overnight in a shaker at 37 °C at 180 r/min. It was transferred to incubate in 300 mL of LB medium (1:100) with 50 μg/mL ampicillin for 2.5 h. The protein expression was induced by the addition of lactose to a final concentration of 2.5 g/mL for 3 h at 37 °C. Cells were collected by spinning at 3000g for 30 min at 4 °C and then resuspended in 10 mL of cell lysis buffer (50 mM Tris-HCl, pH 8.0, 60 μg/mL lysozyme, 0.5% Triton X-100, 10 U/mL DNA enzyme, 1 mM PMSF) per 1 g of

cell. The cell lysate was spun down at 15 000g for 10 min at 4 °C, and the supernatant was filtered with a 0.22 μ m filter. Purification was performed by a GST affinity chromatography column, and elution was done by PBS buffer (KH₂PO₄ 2 mM, Na₂HPO₄ 8 mM, NaCl 136 mM, KCl 2.6 mM) with reduced glutathione (0.154 g/50 mL PBS) to get GST-nNOS₁₋₁₃₃.

The GST-nNOS₁₋₁₃₃ protein was identified by a coomassie blue staining method. The purified and concentrated protein was subjected to SDS-PAGE, dyed with coomassie blue staining solution overnight, and then eluted with the decolorization solution and imaged in white light.

4.2.2. Fluorescence Polarization Assay.^{27,28} Fluorescence polarization experiments were conducted in 96-well, black, flat bottom plates (Corning). The polarization values in milli polarization units (mP) were measured by a plate reader (BMG, LABTECH, POLARstar Omega, Offenburger, Germany). In each well, the final volume was 125 μ L of the PBS buffer (KH₂PO₄ 2 mM, Na₂HPO₄ 8 mM, NaCl 136 mM, KCl 2.6 mM). To determinate the optimal concentration of the free probe (5-FAM-KV-14) for fluorescence polarization assay, the polarization values were tested with increasing concentrations of 5-FAM-KV-14 (from 0.01 nM to 5 μ M). To determine the optimal protein concentration, the GST-nNOS₁₋₁₃₃ concentration was varied from 1 nM to 20 μ M at a fixed concentration of 5-FAM-KV-14 (50 nM). To assay the influence of DMSO, increasing concentrations of 1–8% DMSO were added to the well containing 50 nM 5-FAM-KV-14 and 1 μ M GST-nNOS₁₋₁₃₃. To test the stability, the polarization values were measured at various time points over 24 h.

Z' factor and signal-noise ratio (S/N) statistical experiments were performed to determine the assay quality and suitability in a group (5-FAM-KV-14 bound to GST-nNOS₁₋₁₃₃ and another group (5-FAM-KV-14 alone) in 30 replicates, and experiments were repeated two more times on different days. The Z' factor was calculated using the following equation:

$$Z' = 1 - (3\sigma_{\text{binding}} + 3\sigma_{\text{free}})/|\mu_{\text{binding}} - \mu_{\text{free}}|;$$
$$S/N = (\mu_{\text{binding}} - \mu_{\text{free}})/\sigma_{\text{free}}$$

where σ is the standard deviation, μ is the mean, binding is the FP value of bound 5-FAM- 5-FAM-KV-14 with GST-nNOS₁₋₁₃₃, and free is the FP value of free 5-FAM-KV-14.

Competitive binding experiments were performed by adding increasing concentrations of compounds to a fixed concentration of 5-FAM-KV-14 (50 nM) and GST-nNOS₁₋₁₃₃ domain (1 μ M) at 37 °C for 1 h. All graphs were prepared by GraphPad 7.0 (GraphPad Software, San Diego, CA). All values reported are the average of at least three individual experiments.

4.2.3. Isothermal Titration Calorimetry (ITC).^{29,30} All ITC experiments were performed at 25 °C using an ITC200 microcalorimeter (MicroCal Inc., Northampton, MA) with a 200 μ L cell capacity and a 40 μ L syringe volume. Protein solution (200 μ L) was added to the sample cell. Injections of 2 μ L of ligand (peptides) solution were added at an interval of 2 min into the GST-nNOS₁₋₁₃₃ solution. A reference titration of ligand into buffer was used to correct for the heat of dilution. Finally, all ITC data was analyzed using the Origin 7 software provided by MicroCal.

4.2.4. Molecular Docking Study. The X-ray crystallographic structures of nNOS PDZ (PDB code: 1B8Q) were obtained from the PDB (<http://www.rcsb.org/pdb/>). Discovery Studio (vision 3.5, Accelrys) was used to perform molecular docking. Che-ADAV bound into the three-dimensional structure of nNOS PDZ was carried out following the CDocker protocol.

4.2.5. In Vitro PAMPA-BBB Assay.^{31,32} Carbamazepine and atenolol were elected as the positive and negative controls, respectively. The stock solution of the compounds (5 mg/mL) was prepared in DMSO. The stock solution was diluted to 50 μ g/mL with PBS (1% DMSO) to prepare a test solution. The test solution was added to every donor well (300 μ L per well), and then, the acceptor well was soaked with 5 μ L of porcine polar brain lipid (20 mg/mL) in

dodecane; subsequently, 150 μ L of PBS was added. The acceptor well was placed onto the donor well and incubated at the room temperature for 18 h. The permeability (Pe) was measured using HPLC. After the removal of the acceptor well, the donor/acceptor solutions and standard samples were measured using an Agilent 1200 Infinity Series LC at 235 nm.

4.2.6. Analysis of Che-AD(OMe)AV and Che-ADAV Concentrations in Brain.^{16,33} For pharmacokinetic studies, C57BL/6J mice (20–25 g) were housed individually and fasted overnight before use. Water was allowed *ad libitum*. The concentrations of Che-AD(OMe)AV and Che-ADAV of brain tissue at 1 min, 5 min, 30 min, 45 min, 1 h, and 2 h after intraperitoneal injection (compound AD(OMe)AV, 20 mg/kg,) were measured by HPLC with tandem mass spectrometry (LC–MS). The mice were sacrificed by cervical dislocation, and the brain tissue was rapidly removed at the aforementioned time, rinsed with cold normal saline, and weighed. Then, the whole brain was quickly homogenized on ice using a glass homogenizer and ultrasounded for 10 min. The ice-cold mixture (300 μ L, methanol/acetonitrile = 1:1) along with 10 μ L of the internal standard solution (fluoxetine) mixture were added to 100 μ L of homogenate to precipitate the proteins. The mixture was centrifuged at 10 000g at 4 °C for 10 min, and 20 μ L of the supernatant was injected for LC–MS analysis. The analysis was performed on an Agilent 1200 series LC system using a Sunfire Prep C18 column (4.6 mm \times 250 mm). The mobile phase consisted of 0.1% formic acid in water (A) and acetonitrile (B) (70:30, v/v) with a flow rate of 0.25 mL/min. The detection was carried out with electron spray ionization (ESI) operating at positive ion and multiple reactions monitoring (MRM) mode. Mass parameters including the precursor ion, product ion, fragmentor voltage, and collision energy are shown in Table 3.

4.2.7. Surgical Preparation and Infarct Volume Measurement.^{31,34} Focal cerebral ischemia was performed in male SD rats (Model Animal Research Center of Nanjing University, China) through intraluminal middle cerebral artery occlusion (MCAO) as reported in a method previously. Male SD rats (280–320 g) were randomly divided into four groups (n = 15 per group): (1) sham, (2) vehicle (I/R), (3) I/R + Che-AD(OMe)AV, (4) I/R+edaravone. Under chloral hydrate anesthesia (350 mg/kg, i.p.), a 4/0 surgical nylon monofilament with rounded tip was introduced into the left internal carotid artery through the external carotid stump and advanced 20–21 mm past the carotid bifurcation until a slight resistance was felt. At this point, the intraluminal filament blocked the origin of the middle cerebral artery and occluded all sources of blood flow from the internal carotid artery, anterior cerebral artery, and posterior cerebral artery. Throughout the procedure, the rat body temperature was maintained at 37 \pm 0.5 °C. The filament was left in place for 120 min and then withdrawn for reperfusion. Saline (Sham), saline (vehicle I/R), Che-AD(OMe)AV (10 mg/kg), and edaravone (6 mg/kg) were injected through the tail vein immediately after reperfusion. The infarct volume measurement was performed 24 h after the MCAO as described previously. Brains were removed rapidly and frozen at –20 °C for 5 min. Coronal slices were made at 1–2 mm from the frontal tips, and sections were immersed in 2% 2,3,5-triphenyltetrazolium chloride (TTC; Sigma-Aldrich) at 37 °C for 30 h. The infarct volume was expressed as a percentage of the area of the coronal section in the infarcted hemisphere. The infarct areas (white) in the individual sections were measured and analyzed using Image software.

4.2.8. Statistical Analysis. Data are presented as mean \pm SEM. The data were analyzed by one-way ANOVA followed by *post hoc* Scheffe test. Statistical significance was established at a p value <0.05.

■ ASSOCIATED CONTENT

Supporting Information

The Supporting Information is available free of charge at <https://pubs.acs.org/doi/10.1021/acschemneuro.0c00739>.

Figures of MS, ¹H NMR, and HRMS spectra, reversed-phase HPLC chromatograms, standard curve regression

plots, and chromatograms and table of analytical HPLC data (PDF)

AUTHOR INFORMATION

Corresponding Authors

Yajuan Qin – School of Pharmacy, Nanjing Medical University, Nanjing 211166, China; Phone: +86-25-8686-8486; Email: yjqin@njmu.edu.cn

Tingyou Li – School of Pharmacy, Nanjing Medical University, Nanjing 211166, China; orcid.org/0000-0002-4216-2206; Phone: +86-25-8686-8486; Email: l_tingyou@njmu.edu.cn

Authors

Lingling Feng – School of Pharmacy, Nanjing Medical University, Nanjing 211166, China

Xin Fan – School of Pharmacy, Nanjing Medical University, Nanjing 211166, China

Liping Zheng – School of Pharmacy, Nanjing Medical University, Nanjing 211166, China

Yu Zhang – School of Pharmacy, Nanjing Medical University, Nanjing 211166, China

Lei Chang – School of Pharmacy, Nanjing Medical University, Nanjing 211166, China

Complete contact information is available at:

<https://pubs.acs.org/10.1021/acscchemneuro.0c00739>

Author Contributions

[†]Y.Q. and L.F. contributed equally to this work. Y.Q. and T.L. designed the compounds and the whole study. Y.Q., L.F., and Y.Z. performed the FP assay, analyzed the data, and drafted the manuscript. L.F., X.F., and L.Z. performed the ITC, *in vitro* PAMPA-BBB assay, and *in vivo* pharmacokinetic study. Y.Q. performed the molecular docking study. Y.Q., L.F., and C.L. investigated the neuroprotective ability of the potential compound by MCAO model. Y.Q., L.F., and T.L. drafted the main text of the manuscript. All authors have given their final approval for the manuscript.

Notes

The authors declare no competing financial interest.

ACKNOWLEDGMENTS

This work was supported by the National Natural Science Foundation of China (No. 81803349), Natural Science Foundation of Jiangsu Province (CN) (No. BK20171048).

ABBREVIATIONS LIST

nNOS, neuronal nitric oxide synthases; CAPON (NOSA1AP), carboxy-terminal PDZ ligand of nNOS; FP, fluorescence polarization; ITC, isothermal titration calorimetry; PPI, protein–protein interaction; PDZ, PSD-95, discs large, zonula occludens-1; LC–MS, liquid chromatography–mass spectrometry; DCM, dichloromethane; PBS, phosphate-buffer saline

REFERENCES

- (1) Hu, L., Feng, H., Zhang, H., Yu, S., Zhao, Q., Wang, W., Bao, F., Ding, X., Hu, J., Wang, M., Xu, Y., Wu, Z., Li, X., Tang, Y., Mao, F., Chen, X., Zhang, H., and Li, J. (2020) Development of novel N-hydroxypyridone derivatives as potential anti-ischemic stroke agents. *J. Med. Chem.* 63 (3), 1051–1067.
- (2) Zhang, J., Liu, J., Li, D., Zhang, C., and Liu, M. (2019) Calcium antagonists for acute ischemic stroke. *Cochrane Database Syst. Rev.* 2 (2), CD001928.

- (3) Hiu, T., Farzampour, Z., Paz, J. T., Wang, E. H., Badgely, C., Olson, A., Micheva, K. D., Wang, G., Lemmens, R., Tran, K. V., Nishiyama, Y., Liang, X., Hamilton, S. A., O'Rourke, N., Smith, S. J., Huguenard, J. R., Bliss, T. M., and Steinberg, G. K. (2016) Enhanced phasic GABA inhibition during the repair phase of stroke: A novel therapeutic target. *Brain* 139 (2), 468–480.

- (4) Nakase, T., Yoshioka, S., and Suzuki, A. (2011) Free radical scavenger, edaravone, reduces the lesion size of lacunar infarction in human brain ischemic stroke. *BMC Neurol.* 11 (1), 39.

- (5) Cai, H., Ma, Y., Jiang, L., Mu, Z., Jiang, Z., Chen, X., Wang, Y., Yang, G. Y., and Zhang, Z. (2017) Hypoxia response element-regulated MMP-9 promotes neurological recovery via glial scar degradation and angiogenesis in delayed stroke. *Mol. Ther.* 25 (6), 1448–1459.

- (6) Hertelendy, P., Toldi, J., Fulop, F., and Vecsei, L. (2019) Ischemic stroke and kynurenines: Medicinal chemistry aspects. *Curr. Med. Chem.* 25 (42), 5945–5957.

- (7) Nash, K. M., Schiefer, I. T., and Shah, Z. A. (2018) Development of a reactive oxygen species-sensitive nitric oxide synthase inhibitor for the treatment of ischemic stroke. *Free Radical Biol. Med.* 115, 395–404.

- (8) Bauer, V., and Sotnikova, R. (2010) Nitric oxide—the endothelium-derived relaxing factor and its role in endothelial functions. *Gen. Physiol. Biophys.* 29 (4), 319–340.

- (9) Zhou, L., Li, F., Xu, H. B., Luo, C. X., Wu, H. Y., Zhu, M. M., Lu, W., Ji, X., Zhou, Q. G., and Zhu, D. Y. (2010) Treatment of cerebral ischemia by disrupting ischemia-induced interaction of nNOS with PSD-95. *Nat. Med.* 16 (12), 1439–43.

- (10) Li, L. L., Ginot, V., Liu, X., Vergun, O., Tuittila, M., Mathieu, M., Bonny, C., Puyal, J., Truttmann, A. C., and Courtney, M. J. (2013) The nNOS-p38MAPK pathway is mediated by NOS1AP during neuronal death. *J. Neurosci.* 33 (19), 8185–201.

- (11) Wardlaw, J. M., Murray, V., Berge, E., and del Zoppo, G. J. (2014) Thrombolysis for acute ischaemic stroke. *Cochrane Database Syst. Rev.* 2014 (7), CD000213.

- (12) Zahuranec, D. B., and Majersik, J. J. (2012) Percentage of acute stroke patients eligible for endovascular treatment. *Neurology* 79 (13), S22–5.

- (13) Enomoto, M., Endo, A., Yatsushige, H., Fushimi, K., and Otomo, Y. (2019) Clinical Effects of Early Edaravone Use in Acute Ischemic Stroke Patients Treated by Endovascular Reperfusion Therapy. *Stroke* 50 (3), 652–658.

- (14) Abe, M., Kaizu, K., and Matsumoto, K. (2007) A case report of acute renal failure and fulminant hepatitis associated with edaravone administration in a cerebral infarction patient. *Ther. Apheresis Dial.* 11 (3), 235–40.

- (15) Ni, H. Y., Song, Y. X., Lin, Y. H., Cao, B., Wang, D. L., Zhang, Y., Dong, J., Liang, H. Y., Xu, K., Li, T. Y., Chang, L., Wu, H. Y., Luo, C. X., and Zhu, D. Y. (2019) Dissociating nNOS (neuronal NO synthase)-CAPON (carboxy-terminal postsynaptic density-95/discs large/zona occludens-1 ligand of nNOS) interaction promotes functional recovery after stroke via enhanced structural neuroplasticity. *Stroke* 50 (3), 728–737.

- (16) Zhu, L. J., Li, T. Y., Luo, C. X., Jiang, N., Chang, L., Lin, Y. H., Zhou, H. H., Chen, C., Zhang, Y., Lu, W., Gao, L. Y., Ma, Y., Zhou, Q. G., Hu, Q., Hu, X. L., Zhang, J., Wu, H. Y., and Zhu, D. Y. (2014) CAPON-nNOS coupling can serve as a target for developing new anxiolytics. *Nat. Med.* 20 (9), 1050–4.

- (17) Jaffrey, S. R., Snowman, A. M., Eliasson, M. J., Cohen, N. A., and Snyder, S. H. (1998) CAPON: a protein associated with neuronal nitric oxide synthase that regulates its interactions with PSD95. *Neuron* 20 (1), 115–24.

- (18) Tochio, H., Zhang, Q., Mandal, P., Li, M., and Zhang, M. (1999) Solution structure of the extended neuronal nitric oxide synthase PDZ domain complexed with an associated peptide. *Nat. Struct. Biol.* 6 (5), 417–21.

- (19) Bach, A., Chi, C. N., Olsen, T. B., Pedersen, S. W., Roder, M. U., Pang, G. F., Clausen, R. P., Jemth, P., and Stromgaard, K. (2008) Modified peptides as potent inhibitors of the postsynaptic density-95/

N-Methyl-D-Aspartate receptor interaction. *J. Med. Chem.* 51 (20), 6450–9.

(20) Bach, A., Eildal, J. N., Stühr-Hansen, N., Deeskamp, R., Gottschalk, M., Pedersen, S. W., Kristensen, A. S., and Stromgaard, K. (2011) Cell-permeable and plasma-stable peptidomimetic inhibitors of the postsynaptic density-95/N-Methyl-D-Aspartate receptor interaction. *J. Med. Chem.* 54 (5), 1333–46.

(21) Lim, I. A., Hall, D. D., and Hell, J. W. (2002) Selectivity and promiscuity of the first and second PDZ domains of PSD-95 and synapse-associated protein 102. *J. Biol. Chem.* 277 (24), 21697–711.

(22) Songyang, Z., Fanning, A. S., Fu, C., Xu, J., Marfatia, S. M., Chishti, A. H., Crompton, A., Chan, A. C., Anderson, J. M., and Cantley, L. C. (1997) Recognition of unique carboxyl-terminal motifs by distinct PDZ domains. *Science* 275 (5296), 73–7.

(23) Stiffler, M. A., Chen, J. R., Grantcharova, V. P., Lei, Y., Fuchs, D., Allen, J. E., Zaslavskaya, L. A., and MacBeath, G. (2007) PDZ domain binding selectivity is optimized across the mouse proteome. *Science* 317 (5836), 364–9.

(24) Cabral, J. H. M., Petosa, C., Sutcliffe, M. J., Raza, S., Byron, O., Poy, F., Marfatia, S. M., Chishti, A. H., and Liddington, R. C. (1996) Crystal structure of a PDZ domain. *Nature* 382 (6592), 649–652.

(25) Merino-Gracia, J., Costas-Insua, C., Canales, M. A., and Rodriguez-Crespo, I. (2016) Insights into the C-terminal peptide binding specificity of the PDZ domain of neuronal nitric-oxide synthase. *J. Biol. Chem.* 291 (22), 11581–95.

(26) Fursule, R. A., Patil, P. O., Shewale, B. D., Kosalge, S. B., Deshmukh, P. K., and Patil, D. A. (2009) Novel system for decarboxylative bromination of alpha, beta-unsaturated carboxylic acids with diacetyiodobenzene. *Chem. Pharm. Bull.* 57 (11), 1243–1245.

(27) Nikolovska-Coleska, Z., Wang, R., Fang, X., Pan, H., Tomita, Y., Li, P., Roller, P. P., Krajewski, K., Saito, N. G., Stuckey, J. A., and Wang, S. (2004) Development and optimization of a binding assay for the XIAP BIR3 domain using fluorescence polarization. *Anal. Biochem.* 332 (2), 261–73.

(28) Lei, Y., Hu, T., Wu, X., Wu, Y., Bao, Q., Zhang, L., Xia, H., Sun, H., You, Q., and Zhang, X. (2015) Affinity-based fluorescence polarization assay for high-throughput screening of prolyl hydroxylase 2 inhibitors. *ACS Med. Chem. Lett.* 6 (12), 1236–40.

(29) Wu, D., Liu, D., Zhang, Y., Zhang, Z., and Li, H. (2018) Unravelling the binding mechanism of benproperine with human serum albumin: A docking, fluorometric, and thermodynamic approach. *Eur. J. Med. Chem.* 146, 245–250.

(30) Feng, X., Yu, W., Li, X., Zhou, F., Zhang, W., Shen, Q., Li, J., Zhang, C., and Shen, P. (2017) Apigenin, a modulator of PPAR γ , attenuates HFD-induced NAFLD by regulating hepatocyte lipid metabolism and oxidative stress via Nrf2 activation. *Biochem. Pharmacol.* 136, 136–149.

(31) Shao, C., Yuan, J., Liu, Y., Qin, Y., Wang, X., Gu, J., Chen, G., Zhang, B., Liu, H. K., Zhao, J., Zhu, H. L., and Qian, Y. (2020) Epileptic brain fluorescent imaging reveals apigenin can relieve the myeloperoxidase-mediated oxidative stress and inhibit ferroptosis. *Proc. Natl. Acad. Sci. U. S. A.* 117 (19), 10155–10164.

(32) Malakoutikhah, M., Prades, R., Teixido, M., and Giral, E. (2010) N-Methyl phenylalanine-rich peptides as highly versatile blood-brain barrier shuttles. *J. Med. Chem.* 53 (6), 2354–63.

(33) Chen, D., Zhao, T., Ni, K., Dai, P., Yang, L., Xu, Y., and Li, F. (2016) Metabolic investigation on ZL006 for the discovery of a potent prodrug for the treatment of cerebral ischemia. *Bioorg. Med. Chem. Lett.* 26 (9), 2152–5.

(34) Wang, X., Wang, L., Li, T., Huang, Z., Lai, Y., Ji, H., Wan, X., Xu, J., Tian, J., and Zhang, Y. (2013) Novel hybrids of optically active ring-opened 3-n-butylphthalide derivative and isosorbide as potential anti-ischemic stroke agents. *J. Med. Chem.* 56 (7), 3078–89.